Supplementary Material:
GravoTet: A Fast Multigrid Hierarchy Construction for Tetrahedral Meshes

Anonymous Authors

S1 FDS Linear-Time Complexity

FDS executes a single sweep over the n vertices of the input level, so the outer loop contributes $O(n)$ work. At each vertex, the exclusion check is restricted to the 2-ring neighborhood, which contains at most k vertices. The total work is therefore $O(kn) = O(n)$. We note that k is not bounded a priori for arbitrary mesh connectivity; in practice, all benchmark meshes exhibit bounded vertex valence, and the $O(n)$ scaling is confirmed by the empirical timing results reported in the main paper.

S2 Input Mesh Generation

TetGen is used solely to generate the input tetrahedral meshes; it is not part of the GravoTet hierarchy construction pipeline. We invoke TetGen with quality refinement enabled: a maximum radius-edge ratio of 1.1 and a minimum dihedral angle of 10°, combined with multiple optimization passes to improve element shape. Across all 22 benchmark models, this configuration produced well-shaped input meshes without failures or degenerate elements. The cotangent stiffness matrix S and the barycentric diagonal mass matrix M are assembled using *libigl*.

S3 Further Comparison Details

Per-model comparisons. We present detailed per-model comparison results for all evaluated geometries, sorted by increasing mesh size. Each row shows the rendered input mesh, the M-norm relative residual vs. wall-clock time convergence plot, and the execution time breakdown histogram. These complement the representative example and aggregate metrics in the main paper.

Below we include more detailed relative residual vs. time plots as well as execution time breakdowns for all comparison models. The plots are sorted by increasing mesh size first for the Poisson problem and then for the biharmonic problem.

Hierarchy quality. We report the element quality of each hierarchy level for all comparison models, measured by aspect ratio and minimum dihedral angle (Fig. S5). Each plot shows the distribution across levels for GravoTet. Shi06 does not construct coarse tetrahedral meshes and is therefore not included. Results are sorted by increasing mesh size. Degenerate tetrahedra can occur on coarse levels, and overlapping tetrahedra can occur occasionally. On the tested cube hierarchies, the SAT-confirmed overlap rate stayed below 1% of all tetrahedron pairs on the evaluated coarse levels. This is acceptable in our setting because the coarse levels are used only to define prolongation, while the stiffness and mass matrices are assembled on the input TetGen mesh and the coarse operators are obtained by Galerkin projection.

S4 Robustness of the Prolongation Operator

Overlapping tetrahedra. When multiple coarse tetrahedra overlap, a fine vertex may formally lie inside more than one. The containment search is restricted to tetrahedra incident to the graph-Voronoi seed that owns the fine vertex, so all candidates reside within one coarsening radius. Among these, a single tetrahedron is selected by a fixed, deterministic first-found rule, and the barycentric coordinates of the fine vertex are computed with respect to that tetrahedron, yielding a unique row of P_ℓ. Every candidate produces weights in $[0, 1]$ that sum to one and reproduce affine functions exactly, so the specific choice does not affect solver correctness. In exact local checks, only about 2–5% of local candidate tetrahedron pairs overlapped, although this can involve many coarse tetrahedra because each tetrahedron has many local candidates. Any difference between two competing assignments is bounded by the variation of the coarse field over one coarsening radius, which is below the resolution that level can represent.

Tetrahedron orientation. The barycentric containment test evaluates $\lambda_i = (p - v_j) \cdot \hat{n} \,/\, (v_i - v_j) \cdot \hat{n}$, where $\hat{n}$ is the outward face normal opposite to v_i. If the vertex ordering of a coarse tetrahedron is reversed, both numerator and denominator change sign, leaving the ratio unchanged. The containment condition $\lambda_i \geq 0$ for all i is therefore orientation-independent. Negative signed volume therefore reflects an arbitrary ordering of the newly constructed simplex, rather than a deformation-induced inversion. Only degenerate (zero-volume) tetrahedra are excluded, as the denominator vanishes; these fall back to the lower-dimensional projection described in the main paper.

Poisson Problems

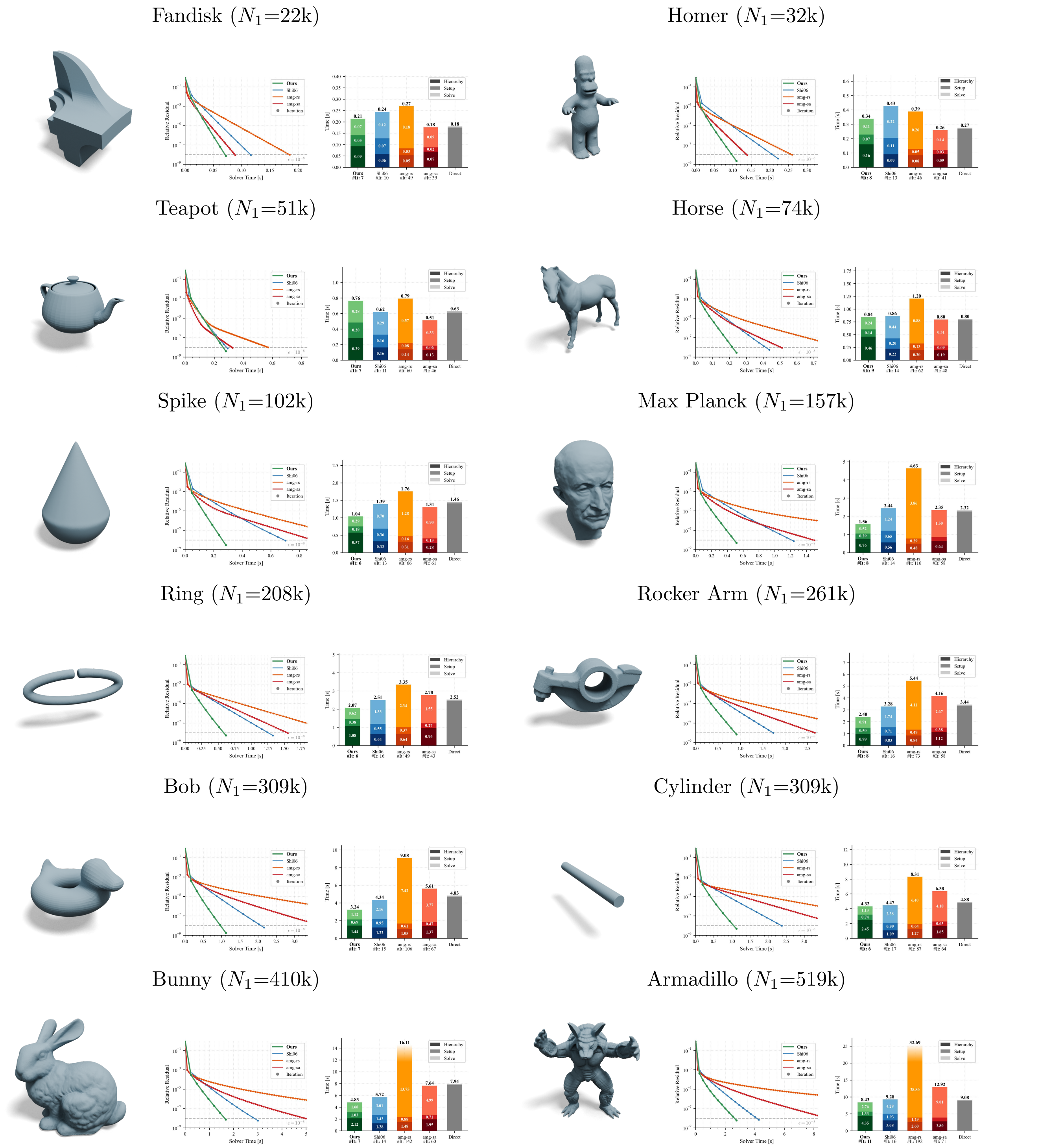

Figure S1: Per-model Poisson solver comparisons (part 1 of 2), sorted by increasing mesh size. Each triplet shows the rendered input mesh (left), relative residual vs. wall-clock time (center), and execution time breakdown (right).

Poisson Problems

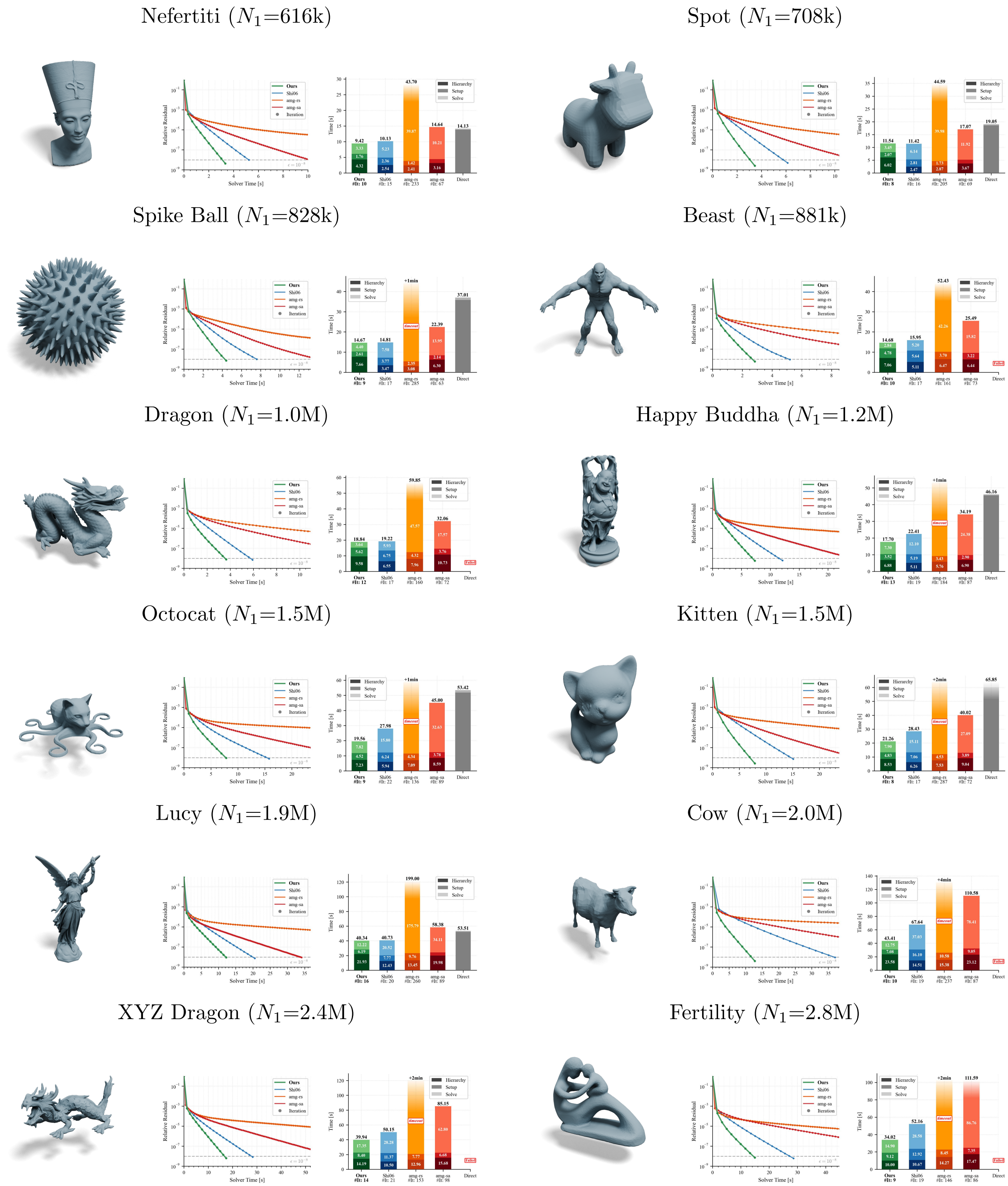

Figure S2: Per-model Poisson solver comparisons (part 2 of 2), continued from the preceding figure. Each triplet shows the rendered input mesh (left), relative residual vs. wall-clock time (center), and execution time breakdown (right). Models are sorted by increasing mesh size.

Biharmonic Problems

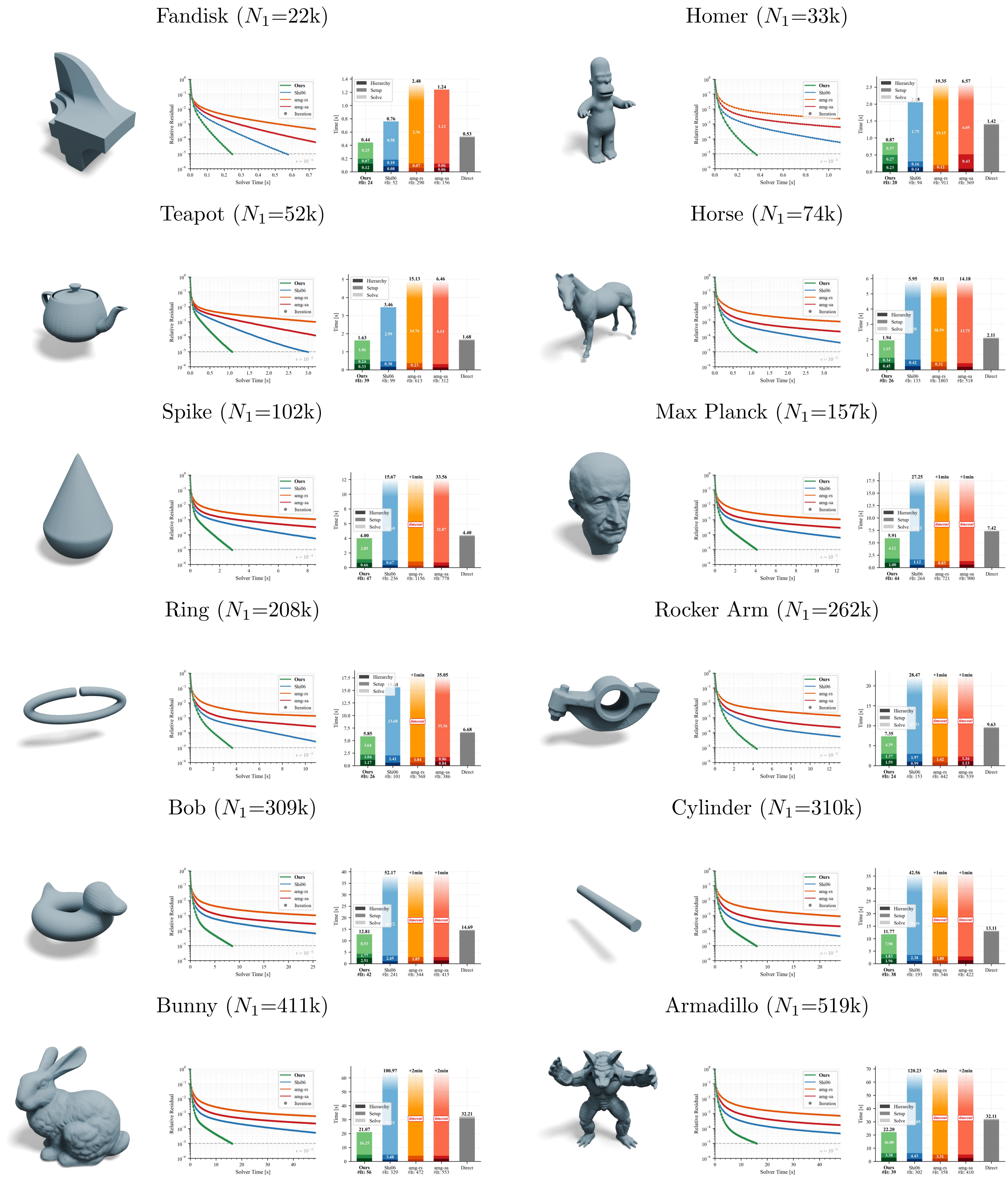

Figure S3: Per-model biharmonic solver comparisons (part 1 of 2), sorted by increasing mesh size. Each triplet shows the rendered input mesh (left), relative residual vs. wall-clock time (center), and execution time breakdown (right).

Biharmonic Problems

Nefertiti (N_1=617k)

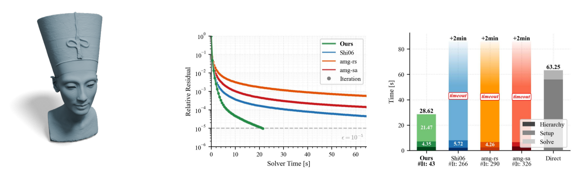

Spot (N_1=709k)

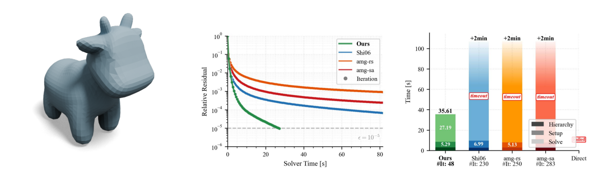

Spike Ball (N_1=829k)

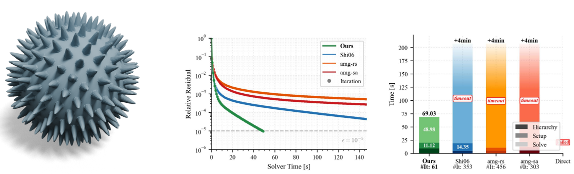

Beast (N_1=881k)

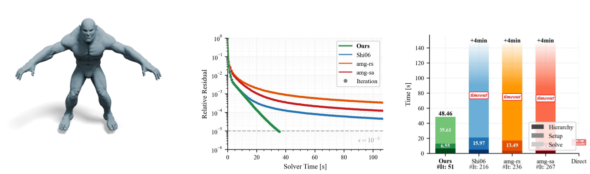

Dragon (N_1=1.0M)

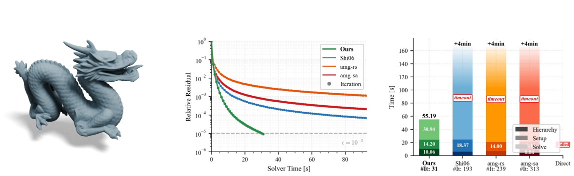

Happy Buddha (N_1=1.2M)

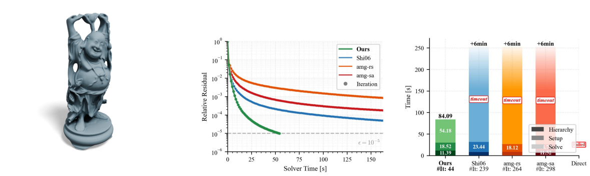

Octocat (N_1=1.5M)

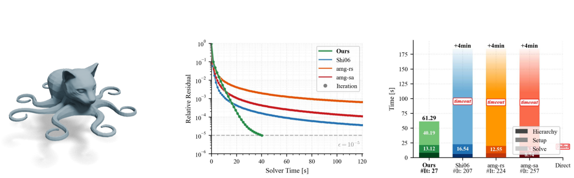

Kitten (N_1=1.5M)

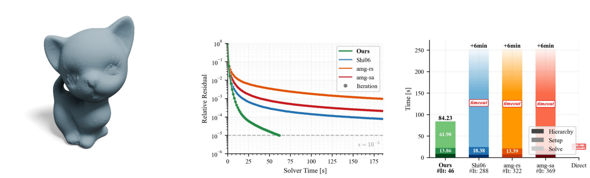

Lucy (N_1=1.9M)

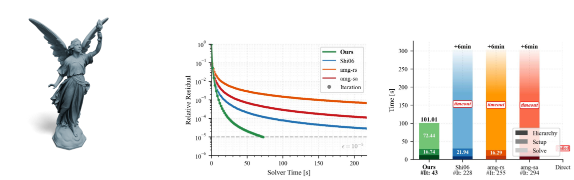

Cow (N_1=2.0M)

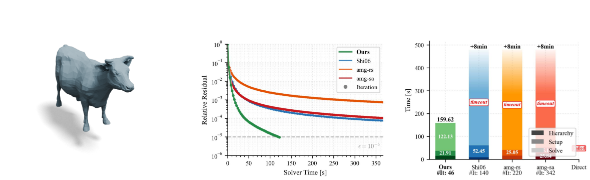

XYZ Dragon (N_1=2.4M)

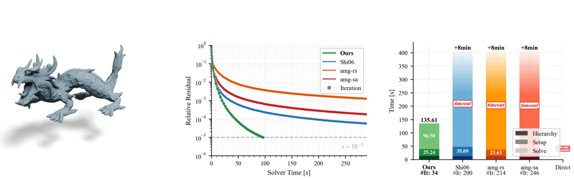

Fertility (N_1=2.8M)

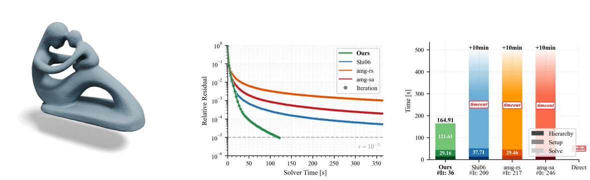

Figure S4: Per-model biharmonic solver comparisons (part 2 of 2), continued from the preceding figure. Each triplet shows the rendered input mesh (left), relative residual vs. wall-clock time (center), and execution time breakdown (right). Models are sorted by increasing mesh size.

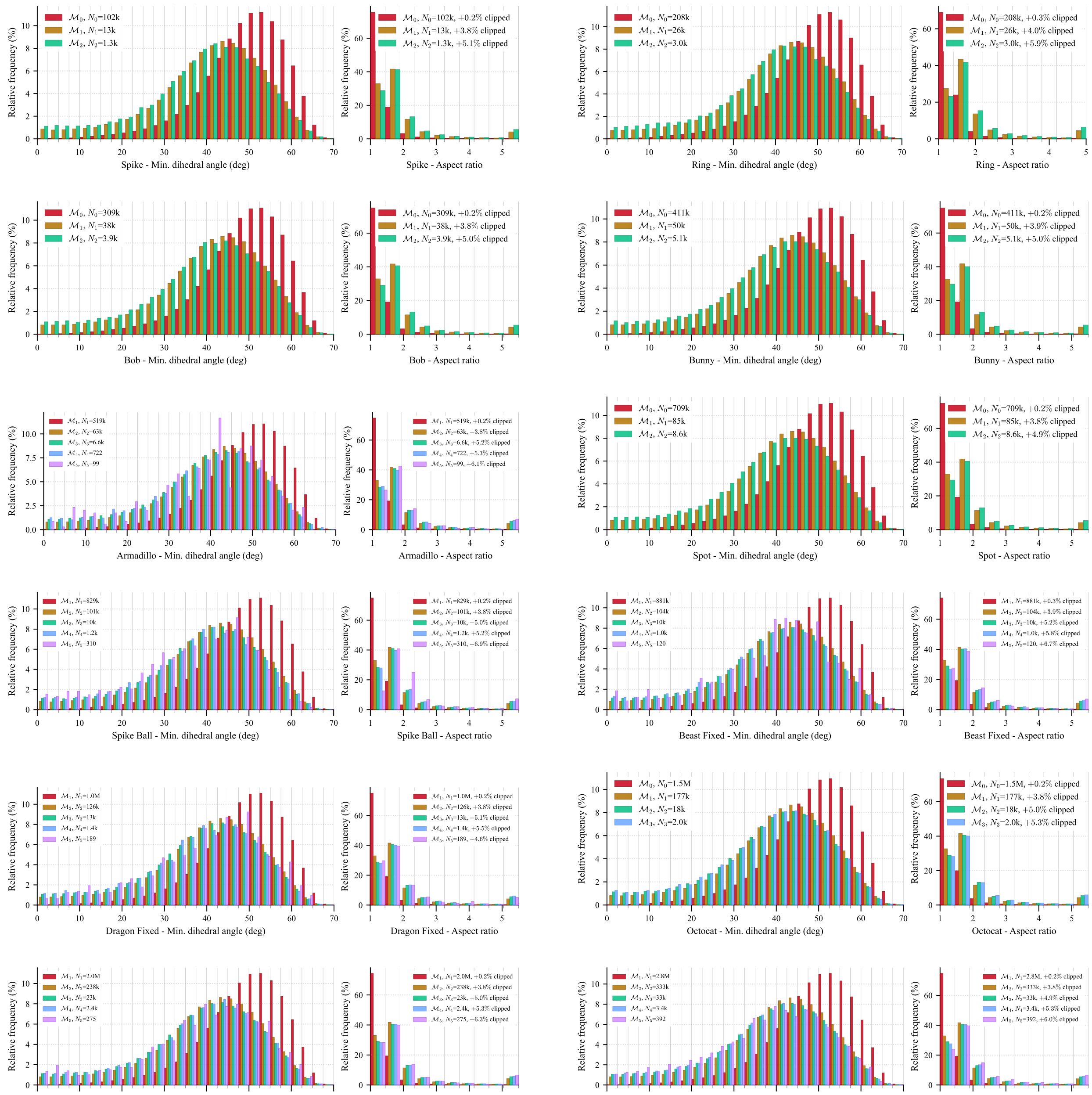

Figure S5: Element quality across hierarchy levels for all comparison models, sorted by increasing mesh size. Each row shows the aspect ratio and minimum dihedral angle distributions per level for GravoTet.